

## Incoherent Matter-Wave Solitons and Pairing Instability in an Attractively Interacting Bose-Einstein Condensate

H. Buljan,<sup>1,2</sup> M. Segev,<sup>1</sup> and A. Vardi<sup>3</sup>

<sup>1</sup>*Physics Department, Technion - Israel Institute of Technology, Haifa 32000, Israel*

<sup>2</sup>*Department of Physics, University of Zagreb, PP 332, Zagreb, Croatia*

<sup>3</sup>*Department of Chemistry, Ben Gurion University of Negev, Beer Sheva 84105, Israel*

(Received 28 August 2004; revised manuscript received 8 April 2005; published 24 October 2005)

The dynamics of matter-wave solitons in Bose-Einstein condensates (BEC) is considerably affected by the presence of a thermal cloud and the dynamical depletion of the condensate. Our numerical results, based on the time-dependent Hartree-Fock-Bogoliubov theory, demonstrate the collapse of the attractively interacting BEC via collisional emission of atom pairs into the thermal cloud, which splits the (quasi-one-dimensional) BEC soliton into two partially coherent solitonic structures of opposite momenta. These incoherent matter waves are analogous to optical random-phase solitons.

DOI: [10.1103/PhysRevLett.95.180401](https://doi.org/10.1103/PhysRevLett.95.180401)

PACS numbers: 03.75.Lm, 03.75.Be, 03.75.Kk, 03.75.Hh

The physics of quantum-degenerate interacting Bose gases closely resembles the behavior of light in nonlinear media. The dynamics of a Bose-Einstein condensate (BEC) at zero temperature is described by the Gross-Pitaevskii (GP) mean-field theory, given by the nonlinear Schrödinger equation for the condensate order parameter. The same equation describes the evolution of coherent light in nonlinear Kerr media. This analogy has opened the way for the field of nonlinear atom optics [1,2] with striking demonstrations of familiar nonlinear optics phenomena such as four wave mixing [3], superradiant Rayleigh scattering [4], and matter-wave amplification [5,6], carried out with matter waves. One such phenomenon is the formation of matter-wave solitons [7–16]. Experimentally, dark solitons [9,10] and bright gap solitons [16] were observed in BECs with repulsive interactions, whereas bright solitons [13,14] were demonstrated in systems with attractive interactions. These experimental results are augmented by extensive theoretical work including predictions on bright [7,8] and dark [11] matter-wave solitons, lattice solitons [12], and soliton trains [15]. The vast majority of previous theoretical efforts on matter-wave solitons have utilized the zero-temperature GP mean-field theory. However, in a realistic system, elementary excitations arising from the thermal and/or quantum fluctuations are always present [17], and the BEC dynamics may be considerably affected by the motion of the excited atoms around it (thermal cloud), and by the dynamical BEC depletion [18], giving rise to new nonlinear matter-wave phenomena.

Here we analyze these aspects of BEC soliton dynamics by using the time-dependent Hartree-Fock-Bogoliubov (TDHFB) theory [19–21]. We focus on bright BEC solitons obtained with attractive interactions between particles. Soliton dynamics is analyzed by first calculating the finite-temperature ground state of the attractively interacting gas within a quasi-one-dimensional (Q1D) cigar-

shaped harmonic trap [17]. The harmonic confinement in the longitudinal direction is then suddenly turned off (the transverse confinement is maintained at all times), and the partially condensed Bose gas starts to evolve. Within the TDHFB model, we find a characteristic pattern of evolution of the system whereby pairs of atoms are collisionally excited from the BEC into the thermal cloud causing the initial density to eventually split into two solitonic structures with opposite momenta. Both solitons constitute a mixture of the condensed and noncondensed particles. We emphasize that the observed composite waves are a truly novel type of matter-wave solitons, where localization is attained not only in spatial density, but also in spatial correlations. These solitons are reminiscent of optical random-phase solitons [22–24], thus highlighting the analogy between incoherent light behavior in nonlinear media and BECs at finite temperatures.

Starting with a near-unity condensate fraction at very low temperatures, the GP dynamics reproduces, under proper conditions, the well-known zero-temperature BEC solitons, thus demonstrating the condensate's mechanical stability. However, the evolution of the same initial nearly pure BEC with TDHFB clearly illustrates BEC depletion through pairing, causing these coherent solitons to disintegrate in a characteristic fashion into incoherent solitary matter waves. In all cases, when both the trap and the interparticle interactions are turned off simultaneously, we observe fast matter-wave dispersion.

We consider a system of  $N$  interacting bosons placed in a Q1D harmonic potential  $V_{\text{ext}}(x, y, z) = (\omega_x x^2 + \omega_{\perp} y^2 + \omega_{\perp} z^2)m/2$ , where  $\omega_{\perp} \gg \omega_x$  denote the transverse and the longitudinal frequencies of the trap, respectively. The interparticle interaction is approximated by the Q1D contact potential  $V(x_1 - x_2) = g_{1D}\delta(x_1 - x_2)$ , where  $g_{1D} = -2\hbar^2/ma_{1D}$ ,  $a_{1D} \approx -a_{\perp}^2/a_{3D}$  is the effective 1D scattering length [25–27],  $m$  is the particle mass,  $a_{\perp} = \sqrt{\hbar/m\omega_{\perp}}$  is the size of the lowest transverse mode, while  $a_{3D}$  is the

3D scattering length. At finite temperatures, the equilibrium state of the system can be described by the HFB theory [17]:

$$H_{sp}\Phi^s + g_{1D}[n_c^s(x) + 2\tilde{n}^s(x)]\Phi^s + g_{1D}\tilde{m}^s(x)\Phi^{s*} = \mu\Phi^s(x), \quad (1)$$

$$\begin{bmatrix} \mathcal{L}^s(x) & \mathcal{M}^s(x) \\ -\mathcal{M}^{s*}(x) & -\mathcal{L}^s(x) \end{bmatrix} \begin{bmatrix} u_j^s(x) \\ v_j^s(x) \end{bmatrix} = E_j \begin{bmatrix} u_j^s(x) \\ v_j^s(x) \end{bmatrix}. \quad (2)$$

Here,  $H_{sp} = -\frac{\hbar^2}{2m}\frac{\partial^2}{\partial x^2} + \frac{1}{2}m\omega_x^2 x^2$  and  $\mu$  is the chemical potential. The superscript  $s$  denotes the static quantities, e.g., the static order parameter is  $\Phi^s(x)$ , and  $n_c^s(x) = |\Phi^s(x)|^2$  is the static condensate density [28]. The normal density is  $\tilde{n}^s(x) = \sum_j |u_j^s(x)|^2 N_j + |v_j^s(x)|^2 (N_j + 1)$ , whereas  $\tilde{m}^s(x) = -\sum_j u_j^s(x)v_j^{s*}(x)(2N_j + 1)$  is the anomalous density [17]. The population of excited modes at temperature  $T$  follows the Bose distribution  $N_j = (e^{E_j/kT} - 1)^{-1}$ . In Eq. (2),  $\mathcal{L}^s(x) = H_{sp} + 2g_{1D}[n_c^s(x) + \tilde{n}^s(x)] - \mu$  and  $\mathcal{M}^s(x) = -g_{1D}[\Phi^{s2}(x) + \tilde{m}^s(x)]$ .

We use the solutions of Eqs. (1) and (2) as the initial conditions to study dynamics without confinement within the TDHFB approximation in the modal form [21]

$$i\hbar \frac{\partial \Phi(x, t)}{\partial t} = H_{sp}\Phi + g_{1D}[n_c(x, t) + 2\tilde{n}(x, t)]\Phi + g_{1D}\tilde{m}(x, t)\Phi^*, \quad (3)$$

$$i\hbar \frac{\partial}{\partial t} \begin{bmatrix} u_j(x, t) \\ v_j(x, t) \end{bmatrix} = \begin{bmatrix} \mathcal{L}(x, t) & \mathcal{M}(x, t) \\ -\mathcal{M}^*(x, t) & -\mathcal{L}(x, t) \end{bmatrix} \begin{bmatrix} u_j \\ v_j \end{bmatrix}, \quad (4)$$

where  $\mathcal{L}(x, t) = H_{sp} + 2g_{1D}[n_c(x, t) + \tilde{n}(x, t)]$ ,  $\mathcal{M}(x, t) = -g_{1D}[\Phi^2(x, t) + \tilde{m}(x, t)]$ ,  $\tilde{n}(x, t) = \sum_j |u_j|^2 N_j + |v_j|^2 (N_j + 1)$  is the normal density, and  $\tilde{m}(x, t) = -\sum_j u_j v_j^* (2N_j + 1)$  is the anomalous density; at  $t = 0$ , all dynamical quantities are identical to their static counterparts, e.g.,  $\Phi(x, 0) = \Phi^s(x)$  etc. The TDHFB model is usually given in the form of coupled equations for the condensate order parameter and the single particle density matrix (e.g., see Ref. [20]). A tedious but straightforward calculation [29] shows its full equivalence to the modal form (4). As expected, when the time dependence of the BEC and quasiparticle functions is  $\Phi(x, t) = \Phi^s(x)\exp(-i\mu t/\hbar)$ ,  $u_j(x, t) = u_j^s(x) \times \exp[-i(E_j + \mu)t/\hbar]$ , and  $v_j(x, t) = v_j^s(x) \exp[-i(E_j - \mu)t/\hbar]$ , the equations of motion (3) and (4) reduce to the static HFB Eqs. (1) and (2).

In what follows we present numerical results based on the described formalism, demonstrating the effect of the thermal atoms and condensate depletion on matter-wave soliton dynamics. The parameters of the calculation are chosen to resemble the experimental parameters of Ref. [13]. We consider  $N = 2.2 \times 10^4$   $^7\text{Li}$  atoms in a cigar-shaped harmonic trap with  $\omega_\perp = 4907$  Hz ( $a_\perp = \sqrt{\hbar/m\omega_\perp} \approx 1.35$   $\mu\text{m}$ ), and  $\omega_x = 439$  Hz ( $a_x = \sqrt{\hbar/m\omega_x} \approx 4.51$   $\mu\text{m}$ ). The 3D scattering length  $a_{3D} = -3.1 \times 10^{-11}$  m corresponds to a nonlinear parameter of

$N|a_{3D}| \approx 0.68$   $\mu\text{m}$ , and is tunable by the Feshbach resonance technique [13].

First we consider the gas prepared at a very low temperature ( $k_B T/\hbar\omega_\perp = 5$ ), where the condensate fraction is 99%. The density of such initially prepared gas  $\approx |\Phi^s(x)|^2$  has a single-humped profile. We have numerically checked the stability [30] of the static confined solution with respect to small perturbations; the stability is underpinned by the use of parameters resembling experiment [13]. When the confinement in  $x$  is turned off (the transverse confinement in  $y$  and  $z$  is maintained), the system is suddenly taken out of equilibrium, and consequently starts to evolve. In the spirit of Ref. [13], we compare the  $x$ -unconfined dynamics of the system in the presence of interactions to its time evolution when both the confinement in  $x$  and the interactions are turned off. The results are shown in Fig. 1. In the absence of interactions we observe fast matter-wave dispersion [Fig. 1(a)]. The dispersion can be counteracted by the attractive particle interactions. The evolution of the

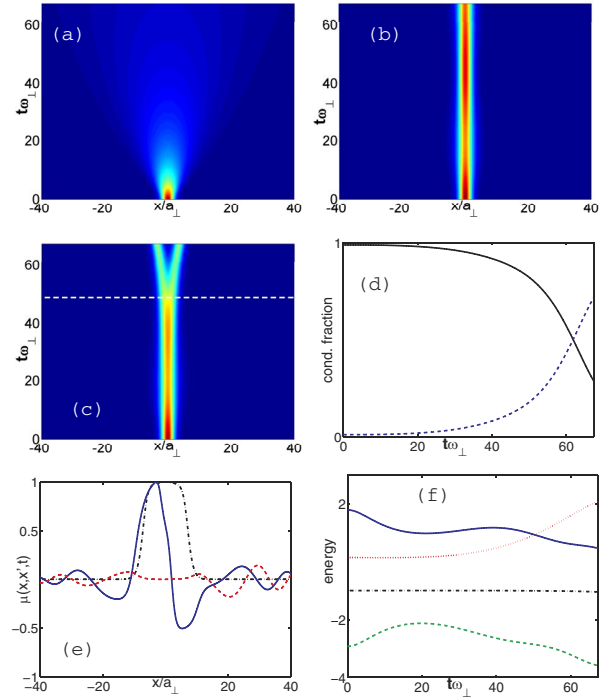


FIG. 1 (color online). (a) Matter-wave dispersion, i.e., evolution of the gas density without interactions present. (b) Coherent matter-wave solitonic evolution with GP equation. (c) Evolution of the gas with the TDHFB model; attractive interactions among atoms are present in figures (b) and (c). (d) The condensate fraction (black solid line) and the fraction of noncondensed atoms (blue dashed line). (e) The complex degree of coherence  $\mu(x, x', t)$  of a matter wave at  $t = 0$  (black dot-dashed line), and  $t\omega_\perp = 63.9$  [Re $\mu(x, x', t)$  blue solid line, and Im $\mu(x, x', t)$  red dashed line];  $x'$  is placed at the position of the left peak. (f) The kinetic energies of the condensate  $E_{\text{kin},c}$  (blue solid line), thermal cloud  $E_{\text{kin},th}$  (red dotted line), and total interaction energy  $E_{\text{int}}$  (green dashed line); total energy  $E_{\text{total}} = E_{\text{kin},c} + E_{\text{kin},th} + E_{\text{int}}$  is conserved (black dot-dashed line); energy is in units of  $|E_{\text{total}}|$ .

initial condition  $\Phi^s(x)$  with the time-dependent GP equation shows mechanically stable solitonic propagation, with small oscillations of the condensate width, rather than a mechanical collapse to a point [Fig. 1(b)]. This motion corresponds to a coherent matter-wave soliton.

However, the evolution of the system with TDHFB equations [Fig. 1(c)] shows that the condensate depletion during the dynamics, and the presence of the noncondensed particles, may considerably affect the motion. The TDHFB model predicts that at some point during the evolution [indicated with the horizontal dashed line in Fig. 1(c)], the single-humped structure of the gas density splits into two solitonic structures with opposite momenta. Figure 1(d) shows depletion of the condensate and increasing population of the thermal cloud during evolution. Because we have initiated the evolution from a low temperature and high condensate fraction, the GP equation describes well the dynamics while  $t\omega_\perp < 40$ ; after this interval the BEC becomes sufficiently depleted and the thermal atoms considerably affect the motion. From Figs. 1(c) and 1(d) we infer that each of the oppositely moving solitonic structures contains both a condensed part and a significant thermal population, i.e., they are partially coherent matter waves. The complex degree of coherence of these waves is expressed by  $\mu(x, x', t) = \rho(x, x', t) / \sqrt{\rho(x, x, t)\rho(x', x', t)}$ , where  $\rho(x, x', t) = \langle \hat{\Psi}^\dagger(x', t)\hat{\Psi}(x, t) \rangle$ , and  $\hat{\Psi}$  is the Bose field operator [17]. Figure 1(e) depicts  $\mu(x, x', t)$  at two different times. The initial matter wave (at  $t = 0$ ) is well correlated, due to the fact that 99% of the particles are condensed, which yields  $\rho(x, x') \approx \Phi^*(x)\Phi(x')$  and  $\mu(x, x') \approx 1$ , corresponding to coherent matter waves [Fig. 1(e)]. However, the BEC is depleted during evolution and correlations become more localized in space [Fig. 1(e)]. It is clearly evident from propagation of the TDHFB equations, allowing BEC depletion, that the BEC collapses via a *pairing* instability [31,32] whereby pairs of atoms are collisionally pulled out of the BEC into the thermal cloud, thus gaining a mean-field energy which goes into their relative motion. This is underpinned in Fig. 1(f) showing the kinetic energies of the condensate  $E_{\text{kin},c} = \int dx \Phi^* \hat{T} \Phi$ , the thermal cloud  $E_{\text{kin},th} = \sum_j \times \int dx \{N_j u_j^* \hat{T} u_j + (N_j + 1) v_j \hat{T} v_j^*\}$ , and the total interaction energy  $E_{\text{int}} = \int dx g \{ \frac{1}{2} |\Phi|^4 + 2n_c \tilde{n} + \tilde{n}^2 + \frac{1}{2} (\Phi^2 \tilde{m}^* + \text{c.c.}) + \frac{1}{2} |\tilde{m}|^2 \}$ ; here  $\hat{T} = -\hbar^2/2m\partial^2/\partial x^2$ . Such pairing collapse with little or no mechanical shrinking is indeed observed in 3D collapse experiments [33,34]. Our results show that in one dimension it results in two partially coherent solitonic structures of opposite momenta. We note that similar structures were observed in stochastic simulations of molecular BEC dissociation in 1D geometry [35], indicating that incoherent matter-wave solitons can also be produced in this system.

While the temperature  $k_B T$  in the previous example is higher than the transverse level spacing  $\hbar\omega_\perp$  whereas a “true” 1D geometry calls for  $k_B T < \hbar\omega_\perp$  [27], the use of a Q1D formalism is still justified because during the evolu-

tion most of the particles are in the condensed phase and in the first few excited modes, which are essentially in one-dimension (they are in the lowest state of the transverse Hamiltonian). Furthermore, only condensed atoms, and the lowest excited modes, determine the outcome of the motion. Therefore, a proper inclusion of the transverse dimension in the calculation would lead to some rescaling of the parameters, but would not influence the dynamics observed in our Q1D calculation. Moreover, the simulations as well as the experiment of [13], are all in the weak interaction regime  $N|a_{1D}|/a_x \sim 10^8 \gg 1$  [25], thus justifying the use of a mean-field approach. The use of the TDHFB approach is further justified by the fact that the system is in the so-called “collisionless regime.” Namely, after the  $x$  confinement is turned off, during a certain relaxation time period, the system would attain equilibrium through collisions. The TDHFB model is inadequate to describe such equilibration of the system. Thus, we can propagate the TDHFB equations only for times much smaller than the relaxation time. As an estimate for the relaxation time we may use the collision time  $\tau_c$  (see, e.g., Ref. [36]). By assuming that the system is in all dimensions confined with the highest trapping frequency  $\omega_\perp$ , the collision time is [36]  $\tau_c \omega_\perp \sim \omega_\perp / (n\sigma v) \sim 10^4$ , where the density is  $n \sim N_{\text{total}}/a_\perp^3$ , the scattering cross section is  $\sigma \sim a_s^2$ , and the velocity is estimated with  $v \sim \sqrt{2\hbar\omega_\perp/m}$ . Clearly, the relaxation time is much larger than the time scale of the pairing instability  $\tau_{\text{p.i.}}$ :  $\tau_{\text{p.i.}} \omega_\perp < 10^2 \ll \tau_c \omega_\perp$ . Thus, starting from a near-zero temperature BEC soliton, GP equation is applicable for a certain time scale, until the BEC depletion and the noncondensed atoms become important; then one may use the TDHFB model. When the condensate fraction becomes sufficiently low, the TDHFB model breaks down, and more accurate theories are required.

Next we consider the system at a higher temperature, where 22% of the particles are initially noncondensed. In this case, the splitting of the initial density into two solitonic structures happens faster than in the previous example [see Fig. 2(a)]. The evolution of the condensate fraction and thermal population is shown in Fig. 2(b). The two splitting peaks are a mixture of the BEC and noncondensed atoms [see Fig. 2(c)]. Figure 2(d) shows localized spatial correlations of solitonic structures. Our incoherent matter-wave solitons are thus rather special in that they correspond to localization of *entropy* and spatial correlation, as well as to localization of density. Note also that the phases of the two separating peaks are well correlated, and  $\pi$  out of phase [Fig. 2(d)], similar to the experiments of Ref. [14], where the relative phase between adjacent solitons in the soliton train was  $\pi$ .

We have observed the process of pairing instability of bright BEC solitons and the formation of incoherent matter-wave solitonic structures in the broad region of the parameter space. In the experiment of Ref. [13], only one single peaked soliton (described by the GP) was observed. This discrepancy may have been caused by the following reason: The experiment of Ref. [13] had an

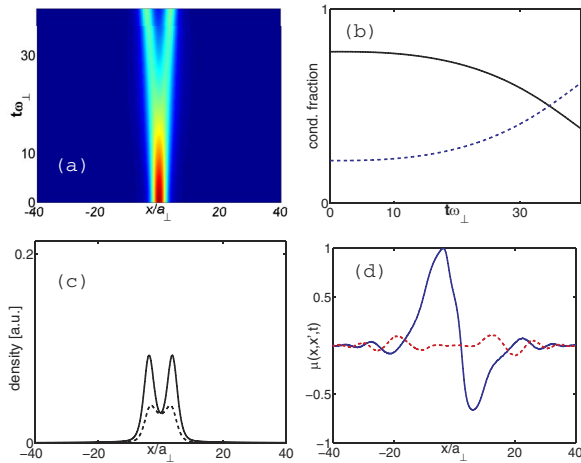


FIG. 2 (color online). (a) Evolution of the gas density with TDHFB. (b) The condensate fraction (black solid line) and the fraction of noncondensed atoms (blue dashed line) during TDHFB evolution. (c) Double peaked total density (solid line), and condensate density (dashed line) at  $t\omega_{\perp} = 37.6$ . (d) The complex degree of coherence  $\mu(x, x', t)$  at  $t\omega_{\perp} = 37.6$  [ $\text{Re}\mu(x, x', t)$  blue solid line, and  $\text{Im}\mu(x, x', t)$  red dashed line];  $x'$  is placed at the position of the left peak.

additional (not negligible) expulsive parabolic potential in the unconfined ( $x$ ) direction, which may considerably alter the behavior of the system. Such potential breaks the symmetry of the system (both static and time evolving), which is of great importance for the observation of the two oppositely moving solitonic structures. In addition, an experiment designed to observe incoherent matter-wave solitons should follow the evolution for sufficiently long times for the pairing instability to set in.

In conclusion, we have used the time-dependent Hartree-Fock-Bogoliubov theory to analyze the influence of the thermal cloud and condensate depletion on the dynamics of bright BEC solitons with attractive particle interactions. We find that the BEC depletion induced by the pairing instability, and the presence of a thermal cloud, cause the particle density to split into two solitonic structures, each being a mixture of the condensed and non-condensed particles. The predicted incoherent matter-wave structures represent novel correlation solitons which resemble localized second-sound entropy waves. They also correspond to incoherent optical solitons [22–24], which points at the analogy between partially condensed Bose gases and nonlinear partially coherent optical waves.

We acknowledge support from the Israel Science Foundation for a Center of Excellence (Grant No. 8006/03). A. V. acknowledges support from the Minerva foundation through a grant for a junior research group.

[1] G. Lenz, P. Meystre, and E. M. Wright, Phys. Rev. Lett. **71**, 3271 (1993).

[2] S. L. Rolston and W. D. Phillips, Nature (London) **416**, 219 (2002).

[3] L. Deng *et al.*, Nature (London) **398**, 218 (1999).

[4] S. Inouye *et al.*, Science **285**, 571 (1999).

[5] M. Kozuma *et al.*, Science **286**, 2309 (1999).

[6] S. Inouye *et al.*, Nature (London) **402**, 641 (1999).

[7] P. A. Ruprecht *et al.*, Phys. Rev. A **51**, 4704 (1995).

[8] V. M. Perez-Garcia, H. Michinel, and H. Herrero, Phys. Rev. A **57**, 3837 (1998).

[9] S. Burger *et al.*, Phys. Rev. Lett. **83**, 5198 (1999).

[10] J. Denschlag *et al.*, Science **287**, 97 (2000).

[11] Th. Busch and J. R. Anglin, Phys. Rev. Lett. **84**, 2298 (2000).

[12] A. Trombettoni and A. Smerzi, Phys. Rev. Lett. **86**, 2353 (2001).

[13] L. Khaykovich *et al.*, Science **296**, 1290 (2002).

[14] K. E. Strecker *et al.*, Nature (London) **417**, 150 (2002).

[15] L. Salasnich, A. Parola, and L. Reatto, Phys. Rev. Lett. **91**, 080405 (2003).

[16] B. Eiermann *et al.*, Phys. Rev. Lett. **92**, 230401 (2004).

[17] A. Griffin, Phys. Rev. B **53**, 9341 (1996).

[18] Y. Castin and R. Dum, Phys. Rev. Lett. **79**, 3553 (1997).

[19] N. P. Proukakis and K. Burnett, J. Res. Natl. Inst. Stand. Technol. **101**, 457 (1996); N. P. Proukakis, K. Burnett, and H. T. C. Stoof, Phys. Rev. A **57**, 1230 (1998).

[20] M. Holland, J. Park, and R. Walser, Phys. Rev. Lett. **86**, 1915 (2001).

[21] A. M. Rey *et al.*, Phys. Rev. A **69**, 033610 (2004); appendix A of that paper contains the modal form of TDHFB in the discrete Bose-Hubbard model.

[22] M. Mitchell *et al.*, Phys. Rev. Lett. **77**, 490 (1996); M. Mitchell and M. Segev, Nature (London) **387**, 880 (1997).

[23] D. N. Christodoulides *et al.*, Phys. Rev. E **63**, 035601 (2001).

[24] M. Mitchell *et al.*, Phys. Rev. Lett. **79**, 4990 (1997).

[25] V. Dunjko, V. Lorent, and M. Olshanii, Phys. Rev. Lett. **86**, 5413 (2001).

[26] K. V. Kheruntsyan *et al.*, Phys. Rev. Lett. **91**, 040403 (2003).

[27] H. Moritz *et al.*, Phys. Rev. Lett. **91**, 250402 (2003).

[28] While strictly speaking the 1D critical temperature is  $T_c = 0$ , there is significant increase in the population of the lowest energy state below  $k_B T_c = \hbar\omega_x N / \ln(2N)$ ; see W. Ketterle and N. J. van Druten, Phys. Rev. A **54**, 656 (1996).

[29] H. Buljan *et al.* (unpublished).

[30] Yu. Kagan, A. E. Muryshev, and G. Schlyapnikov, Phys. Rev. Lett. **81**, 933 (1998).

[31] W. A. B. Evans and Y. Imry, Nuovo Cimento B **63**, 155 (1969).

[32] G. S. Jeon, L. Yin, S. W. Rhee, and D. J. Thouless, Phys. Rev. A **66**, 011603 (2002).

[33] E. A. Donley *et al.*, Nature (London) **412**, 295 (2001).

[34] J. N. Milstein, C. Menotti, and M. J. Holland, New J. Phys. **5**, 52 (2003).

[35] K. V. Kheruntsyan and P. D. Drummond, Phys. Rev. A **66**, 031602 (2002).

[36] Yu. Kagan, E. L. Surkov, and G. V. Shlyapnikov, Phys. Rev. A **54**, R1753 (1996).